American Mineralogist, Volume 91, pages 816–825, 2006

Dehydroxylation, proton migration, and structural changes in heated talc: An infrared spectroscopic study

MING ZHANG,[1,*] QUN HUI,[1] XIAO-JIE LOU,[1] SIMON A.T. REDFERN,[1] EKHARD K.H. SALJE,[1] AND SERENA C. TARANTINO[2]

[1]Department of Earth Sciences, University of Cambridge, Downing Street, Cambridge CB2 3EQ, United Kingdom
[2]Dipartimento di Scienze della Terra, Università di Pavia, via Ferrata 1, I-27100 Pavia, Italy

ABSTRACT

The high-temperature dehydroxylation and structural change of talc, $Mg_3(Si_2O_5)_2(OH)_2$, has been investigated in detail using infrared (IR) spectroscopy. The data (in the region of 20–12000 cm^{-1}) on quenched samples show that absorptions from structurally incorporated OH and OD, as well as NH_4-like species, have similar temperature dependences in dehydroxylation. The OH species exhibit weak variation in frequency on heating, which is inconsistent with thermally induced weakening of O-H bonds. Dehydroxylation in talc is a complex process that involves proton migrations and formation of new OH species. Additional fundamental OH bands near 3665 and 3745 cm^{-1} became detectable near 900 °C. On further heating the former disappear near 1200 °C, whereas the latter became undetectable near 1350 °C. The occurrence of CO_2 is observed in samples quenched between 600 and 1250 °C. The phonon spectrum (20–1500 cm^{-1}) of the dehydroxylate (obtained by annealing the sample at 1000 °C) gives features significantly different from that of talc, indicating the loss of the original layer structure. The IR data imply that the talc dehydroxylate consists of disordered SiO_2 and enstatite ($MgSiO_3$). Although $MgSiO_3$ exists dominantly in the form of orthoenstatite, the characteristic bands of clinoenstatite phase are found to coexist in the samples treated at 1000 °C. The IR data from in situ measurements show that protons become mobile at temperatures below the dehydroxylation and an extra OH species near 3500 cm^{-1} develops on heating. This new species is not quenchable, and it decreases intensity on cooling and disappears at room temperature. The in situ results also indicate external carbon-related substances can diffuse into talc during dehydroxylation.

Keywords: Infrared spectroscopy, talc, dehydroxylation, OH, OD, NH_4, CO_2, enstatite

INTRODUCTION

Talc is a magnesium tetrasilicate with the formula $Mg_3(Si_2O_5)_2(OH)_2$. Structurally, it belongs to 2:1 trioctahedral phyllosilicates. The crystal consists of an octahedral layer with Mg^{2+} between two silicate tetrahedral layers in which each SiO_4 shares three corners with the adjacent tetrahedra. Talc has found wide applications, such as an ingredient in ceramics, paper, paint, roofing, plastics, cosmetics, talcum, and baby powders. It is also used in the production of refractories and in the manufacture of fireproof paints. Therefore, it is important to gain a good understanding of the thermal behavior of talc.

This present investigation of talc is also inspired by the question of what happens at the atomic level during dehydroxylation of layer silicates and clay minerals. Dehydroxylation in phyllosilicates has attracted very many investigations, and several different mechanisms have been proposed (e.g., MacKenzie et al. 1985; Guggenheim et al. 1987; Drits et al. 1995; Fitzgerald et al. 1996; Bray and Redfern 1999; Muller et al. 2000; Wang et al. 2002, Sainz-Díaz et al. 2004; Zhang et al. 2005). However, how dehydroxylation is initialized, for example by proton or hydroxyl migration, remains unclear. There is a general lack of detailed analysis of the behavior of hydroxyl species and other phonon bands at high temperatures. In particular, the analytical methods employed in some previous investigations did not directly monitor the change of hydroxyls, and some of these results are very likely to be the combinations of dehydroxylation and other thermally induced processes. For talc, in spite of extensive investigations, the dehydroxylation process and the final products reported by previous studies remain unclear. There have been controversies over some of the results reported previously (see Wesolowski 1984 for reviews). The differences can be summarized into three types. (1) Thermogravimetric results of talc at high temperatures are not fully consistent in terms of numbers of endothermic peaks and their temperatures. As the differences in some reported results are so significant, it raises a question: whether the reported loss is really related to dehydroxylation or dehydration and whether some losses are simply due to other process e.g., gas release or dehydroxylation of impurities. (2) Different stages of talc dehydroxylation have been reported: one stage (e.g., Bošković et al. 1968; Ward 1975), two stages (e.g., Ishii et al. 1974), and three stages (e.g., Avgustinik et al. 1948). It has been shown that in vacuum the dehydroxylation of talc begins at a temperature about 100 °C lower than that observed in air (Krönert et al. 1964a, 1964b). Krönert et al. (1964a) have reported that the presence of other minerals can speed up the

* E-mail: mz10001@esc.cam.ac.uk

decomposition of talc and the formation of new phases. (3) Different phases (proto, ortho, clinoenstatite) were observed in the dehydroxylated talc and reported results differ. In the present study, we employed IR spectroscopy to directly monitor the behaviors of OH species as well as other vibrations (e.g., Si-O, and Mg-O) in talc. The results show that the dehydroxylation in talc is a complex process involving the migration of protons at temperatures far below the commonly reported dehydroxylation, the formation of new OH species and decomposition of talc into different phases.

Experimental methods

Two talc samples were measured in this study. One sample (GLS01) originates from Longshen, Guangxi Province, China, and the other (LHC01) from Haicheng, Liaoning Province, China. Electron microprobe analysis shows that the two samples have almost ideal chemical compositions of talc (Table 1). Both powdered (with grain sizes of a few micrometers) and thin section (with thickness of 80~324 μm) samples were used in the experiments. The thermal treatment of the talc sample was carried out between 300 and 1400 °C in a Lenton furnace in air at one atmosphere. The furnace was pre-heated to the set temperature before sample loading and the samples were annealed for 15 min (for the thin sections) or 1 h (for powdered samples). The annealing time was chosen to gain a better understanding of the effect of temperature on the samples. Treated samples were quenched onto lab benches in air. Fresh sample powders were used for the treatment at different temperatures, however, thermally treated thin sections were subsequently annealed at a higher temperature after being measured at room temperature. The pellet technique reported by Zhang et al. (1996) was used to measure the powdered samples. Polyethylene and KBr powders were used as matrix materials (the weight ratio of sample to matrix = 1:50 for polyethylene, and 1:300 or 1:100 for KBr). The sample/matrix mixtures were pressed into disk-shaped pellets of 13 mm diameter at room temperature under vacuum. The sample pellets prepared with KBr were then stored in an oven (150 °C) for 2 h to remove possible absorbed surface water. A gem-quality orthopyroxene (enstatite, $MgSiO_3$) sample Birm2 (the crystal chemical characterization of the sample is given by Tarantino et al. 2002a), originating from Birmania, was measured for comparison. Two single crystals were oriented using a conventional Philips PW1100 four-circle diffractometer. Once the orientation was determined, glass needles were glued to the crystals to embed them in epoxy and to prepare two thin sections (80–100 μm) with *a** and *b** perpendicular to the mounting, respectively. Finally, both sides of sections were polished.

Two spectrometers—Bruker IFS 113v and Bruker IFS 66v—were used for collecting absorption spectra between 20 and 12000 cm^{-1}. Far and mid IR data were recorded using the Bruker IFS 113v spectrometer. For the far IR measurements of polyethylene pellets, a DTGS detector with a polyethylene window, 6 μm Ge-coated and 25 μm Mylar beamsplitters and a Mercury lamp were used. The mid IR measurements between 350 and 5000 cm^{-1} were conducted on KBr pellets. For this frequency region, a DTGS detector with a KBr window, a KBr beamsplitter and a Globar lamp were chosen. Absorption data between 2000–12000 cm^{-1} were obtained from thin section samples using the Bruker IFS 66v spectrometer. A liquid-nitrogen-cooled MCT detector, a KBr or CaF_2 beamsplitter and a tungsten lamp were employed. For in situ high-temperature measurements, the thin section samples were placed in a cylindrical platinum-wound furnace in the spectrometer's sample chamber. The sample temperature was measured using a Pt/PtRh thermocouple placed against the samples. Heating rate was 15 °C/min. IR data were recorded on both heating and cooling runs. All the IR measurements were carried out under vacuum to avoid absorption from water and carbon oxides in the air.

Results

IR spectrum of talc

The vibrational bands of talc and other layered silicates have been reported in earlier studies (Farmer and Russell 1964; Ishii et al. 1967; Wilkins and Ito 1967; Russell et al. 1970; Farmer 1974; Martin et al. 1999; Petit et al. 2004). However, the present study presents to date the most complete IR data set of talc recorded in the range of 20 and 12000 cm^{-1} [the far IR (FIR) to the near IR (NIR)]. The features in the FIR region are mainly due to interlayer vibrations (Fig. 1a), whereas the features between 250 and 600 cm^{-1} are related to tetrahedral bending, Mg-O and OH bands (Fig. 1b). The stretching vibrations of SiO_4 tetrahedra and Si-O-Si linkage are located between 800 and 1200 cm^{-1}. The absorption associated fundamental OH vibrations have been recognized through hydrogen-deuterium substitution experiments (e.g., Russell et al. 1970; Martin et al. 1999). In the frequency region below 1200 cm^{-1}, the talc samples show OH bands near 260, 465, 538, and 669 cm^{-1}. The bands near 260 and 538 cm^{-1} are attributed to the octahedral oxygen and hydroxyls vibrations. The 465 cm^{-1} band is mainly due to the translational motion of the hydroxyl group. The band near 669 cm^{-1} is attributed to OH^- libration. The two samples studied both have a weak absorption feature near 781 cm^{-1}. This band is considered as absorption feature related to OH species. Although this band is not widely reported in natural talc, synthetic Ge-bearing Mg/Ni/Co talc samples have a feature between 700 and 800 cm^{-1}, which exhibits a frequency decrease (with a frequency ratio $\omega_H/\omega_D \approx 1.35–1.36$) after deuteration (Martin et al. 1999). Sample LHC01 shows a sharp absorption

Table 1. Electron microprobe analyses of talc samples

Sample	MgO	SiO_2	Al_2O_3	FeO	CaO	K_2O	Na_2O	TiO_2
LHC01	30.77	63.84	0.05	0.02	0.03	0.01	0.01	–
GLS01	30.56	63.58	0.06	0.60	0.04	0.01	0.01	–

Note: – = undetectable

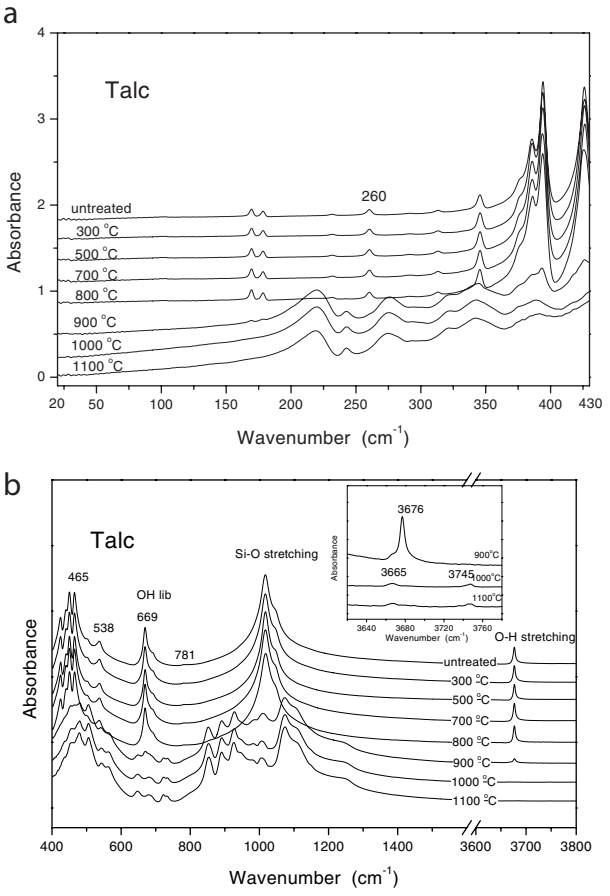

Figure 1. Temperature evolution of vibrational bands of talc (sample LHC01): (**a**) 20–430 cm^{-1} (from polyethylene pellets) and (**b**) 350–4500 cm^{-1} (obtained from KBr pellets). The spectra are shifted for clarity.

with a full width at half maximum of 5 cm^{-1} near 3676 cm^{-1} (Figs. 1b and 2a). High-resolution IR measurements (with instrumental resolutions of 0.1 and 0.2 cm^{-1}) at 20 K revealed that this feature in fact consists of three individual bands separated by a frequency difference of about 2 cm^{-1} (low-temperature IR data will be published separately). In ideal talc, the hydroxyl ion is believed to be symmetrically linked to three Mg ions, and this 3676 cm^{-1} band has been assigned as O-H stretching associated with the Mg_3OH species (Wilkins and Ito 1967; Petit et al. 2004). The IR spectra between 4000 and 4500 cm^{-1} consist of several features (4055, 4182, 4323, and 4369 cm^{-1}), which have complex origins (Fig. 3a). Their frequencies indicate that they must be related to multi-phonon processes, but they are not simply due to three-phonon processes of the vibrations (e.g., Si-O, Mg-O, O-Si-O) related to the framework of talc as their intensities are about 50% of those of the second overtone of Si-O vibrations between 1600 and 2100 cm^{-1} (absorption signals from three-phonon processes are expected to be one or two order of magnitude less intense than those in two-phonon process). These bands are mainly attributed to combinations of the O-H stretching bands (near 3676 cm^{-1}) with other OH^- vibrations (e.g., the OH bands near 781, 670, 538, and 465 cm^{-1}), as the bands between 4100 and 4600 cm^{-1} disappeared in the talc dehydroxylate and their frequencies are basically consistent with the sum of the individual phonons. The feature near 7185 cm^{-1} (Fig. 3b) is assigned as the first overtone of the O-H stretching band located near 3676 cm^{-1}, whereas the band near 10535 cm^{-1} is attributed to its second overtone (Fig. 3c). Although samples LHC01 and GLS01 show essentially identical IR spectra between 20 and 1500 cm^{-1}, the latter has an extra O-H stretching band near 3660 cm^{-1} (Fig. 2b), as well as its overtone bands near 7153 and 10481 cm^{-1}. This 3660 cm^{-1} feature is related to the substitution of Mg by Fe in talc, i.e., this band is assigned to the $(Mg_2, Fe)OH$ vibration (e.g., Petit et al. 2004). This observation is also consistent with the chemical analysis, as sample GLS01 has a higher Fe concentration (Table 1). Although the natural deuterium/hydrogen ratio is very low ($D/H \approx 1.5 \times 10^{-5}$), our measurements from the thin section samples (with thickness of 100–300 μm) were able to reveal the existence of deuterium. As shown in Figure 4, the presence of deuterium in samples is evidenced by the characteristic O-D stretching band near 2710 cm^{-1}. Its frequency agrees very well with that of OD vibrations observed in hydrogen-deuterium exchanged talc (Ferrage et al. 2003). The detection of the OD feature in these natural talc samples also indicates the high sensitivity and good quality of the IR data reported by the present investigation. Although absorbed H_2O is common in natural clays, the IR data from the talc thin sections show essentially a flat line between 5000 and 5500 cm^{-1}, indicating the lack or absence of the combination band (stretching + bending vibrations) of H_2O, i.e., the lack of H_2O species in the starting materials.

Unexpected features were observed near 2980, 3020, 3048, and 3169 cm^{-1} in thin sections of the two talc samples (Figs. 5a and 5b), although they are too weak to be resolved in the pellet samples, which contains much smaller amount of the sample materials. These features are not due to the typical absorption near 2850 and 2960 cm^{-1} from FT-IR spectrometers, because they have different frequencies, showed consistent intensities and disappeared above 950 °C (see a later section). Micro-IR analysis

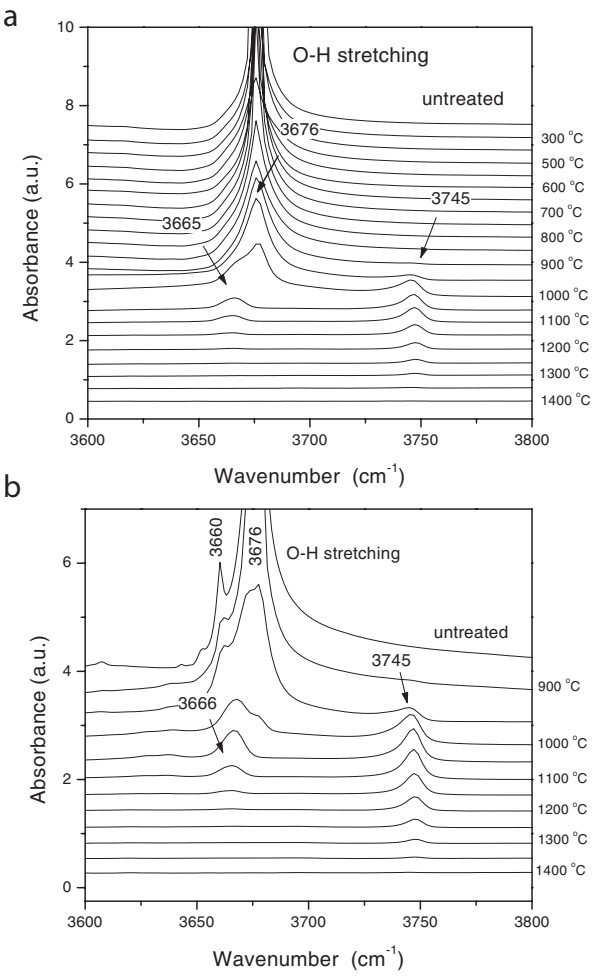

FIGURE 2. Temperature evolution of IR spectra of fundamental OH bands between 3600 and 3800 cm^{-1} (data from thin sections): (**a**) sample LHC01 and (**b**) sample GLS01. The spectra are shifted for clarity. The 3660 cm^{-1} band in GLS01 is due to the substitution of Mg by Fe. Additional signal near 3665 and 3745 cm^{-1} appeared between 900 and 1350 °C.

(beam size = 20 μm) showed that these features have similar intensities from area to area, suggesting that they are not due to inclusions or impurity phases. The vibrational origins of the bands near 2980, 3020, 3048, and 3169 cm^{-1} are not apparently clear. Although C-H vibrations of CH_n (e.g., CH_3 and CH_4) could also appear in this wavenumber region, the presence of these bands at temperatures as high as 800 °C in annealed samples (see earlier sections) does not favor the idea, as CH_n species are commonly volatilized at much lower temperatures. The frequencies of these features are consistent with the characteristic bands of N-H stretching of NH_4^+. Further IR and Raman measurements were carried out to check the possible presence of the bending vibrations (ν_2 and ν_4 near 1400 and 1600 cm^{-1}, respectively) of NH_4^+. IR data form thin sections showed multi-phonon bands between 1600 and 2100 cm^{-1} that made determining the ν_2 and ν_4 bands of NH_4^+ difficult. A band near 1450 cm^{-1} and another one near 1648 cm^{-1} were also recorded in micro-Raman spectrum. These Raman

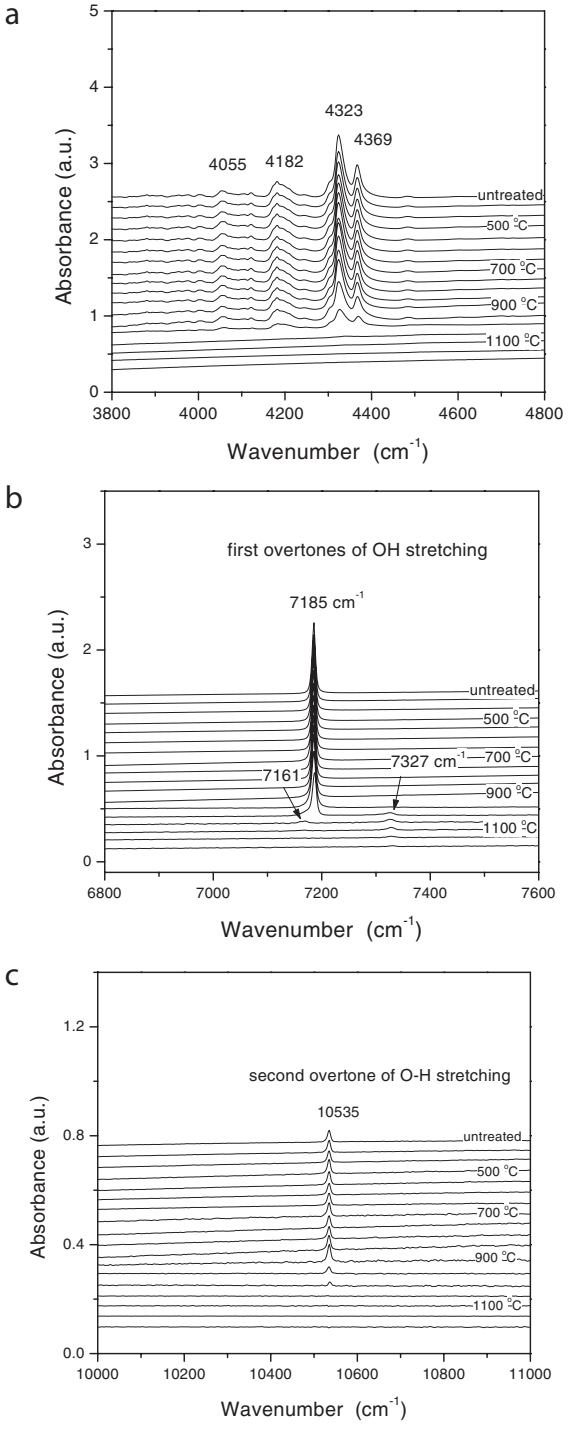

FIGURE 3. Temperature evolution of multi-phonon bands associated with OH (data from thin sections of LHC01): (**a**) combination bands between 3800 and 4800 cm^{-1}; (**b**) first overtones of O-H stretching (between 6800 and 7600 cm^{-1}); and (**c**) second overtones of O-H stretching vibrations. The spectra are shifted for clarity. Additional signal near 7161 and 7327 cm^{-1} appeared between 900 and 1350 °C.

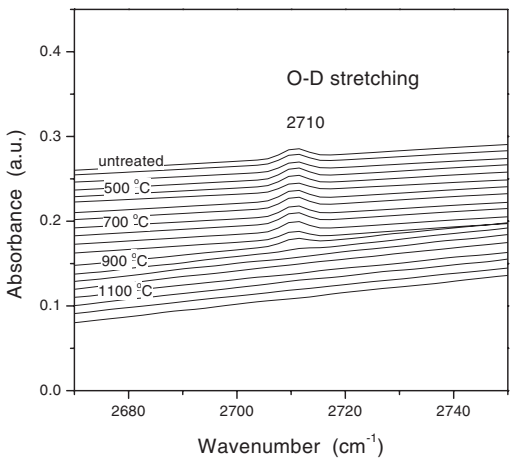

FIGURE 4. Temperature evolution of OD spectra of talc LHC01 (data from thin sections).

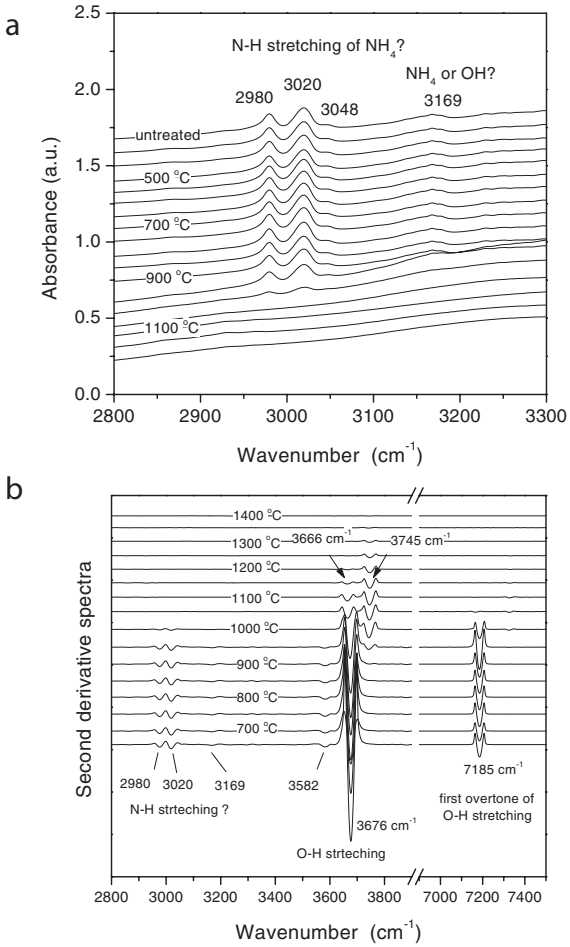

FIGURE 5. Temperature evolution of NH_4-like species (data from thin sections of LHC01): (**a**) absorption spectra, and (**b**) second derivative spectra. The spectra are shifted for clarity.

bands, which are attributed the characteristic bending vibrations of NH_4^+, are accompanied by Raman features between 2800 and 3000 cm^{-1}, which are consistent with N-H stretching vibrations. The observation of these Raman bands appears to support the presence of NH_4^+ in the untreated materials, however, in situ IR measurements (see a later section) revealed an unusual increase

in intensity of these IR bands during heating. We phrased these bands as NH_4^+-like species because of their possible complex origins. Although we were not aware of previous analysis of NH_4^+ in talc prior to the present observation, this ion has been reported in other layer silicates (e.g., kaolinite by Bishop et al. 2002; muscovite by Busigny et al. 2003; smectite and illite reported by Pironon et al. 2003; and vermiculite reported by Pérez-Rodríguez et al. 2004). Comparing the IR intensity of NH_4^+-like species in the talc samples with those in the calibration for muscovite by Busigny et al. (2003) implies estimated NH_4^+ concentrations of tens to hundreds of ppm in LHC01 and GLS01. We did not detect CO_3, CO_2, and CO species in the starting materials (Figs. 1b and 6).

Results of quenched samples

Heating the samples to high temperatures led to dehydroxylation and structural modifications. At temperatures below 800 °C, the thermal treatments did not result in significant changes in spectral features of OH, OD, and NH_4^+-like species (Figs. 1–5). The samples heated at 850 °C showed relatively low IR intensity for the Mg_3OH species near 3676 cm^{-1}, accompanied by changes in the spectral patterns (Figs. 1b, 2a, and 2b). The 3660 cm^{-1} band of (Mg_2, Fe)OH vibration and its overtones showed thermal behavior essentially identical to that of the Mg_3OH vibration (Figs. 2b and 3b). The OD species in talc showed similar thermal behavior as those of OH species. The band area of the OD feature near 2710 cm^{-1} decreases dramatically between 850 and 900 °C (Fig. 4), consistence with the behavior of OH species. The process is better seen in Figures 7a–7c, where the temperature dependences of the integral absorbance for different species are given. As the fundamental OH band near 3676 cm^{-1} has a very large absorption coefficient and it is difficult to record it for thin sections, the data on OH species used in Figure 7a were obtained by integration of the OH combination bands near 4300 cm^{-1}. In partially dehydroxylated talc heated above 900 °C, we observed the formation of two additional bands near 3665 and 3745 cm^{-1} (Figs. 2a and 2b), together with their first overtones near 7161 and 7327 cm^{-1} (Fig. 3b). Both bands appeared in powdered and thin section samples. We were unable to detect their second overtone near 10 500 cm^{-1} because of their low intensity. On further heating, these two extra bands showed a systematic increase in intensity (Figs. 2a, 2b, and 8a). We are not aware of any previous reports of these two bands in heated talc. Their revelation by the present study is probably due to the high quality of our data, although they have low intensity. These two extra bands are assigned to the vibrations associated with new OH species in the dehydroxylated or partially dehydroxylated talc. It is surprising that the additional band near 3665 cm^{-1} did not vanish until heating to 1250 °C. The 3745 cm^{-1} band became undetectable on heating to1350 °C. The loss rate and/or increase rate of these original or extra OH species are better indicated in Figure 9a by the derivative of band integral absorbance shown in Figure 8a. The negative values in Figure 9a correspond to decreases in intensity or concentrations and positive values indicate increases in concentrations. We noted that on approaching dehydroxylation the recorded band intensity of the first overtone near 7185 cm^{-1} and the second overtone near 10535 cm^{-1} both showed an anomaly, a slight increase in intensity with different degrees from 900 and 950 °C, in contrast to the behavior of the fundamental and combination bands of the OH species. This may be due to the change of absorption coefficients for the bands, or the possible formation of small cages or voids during dehydroxylation and the damaged surface as a direct result of degassing, which scatter the incident light. This observation

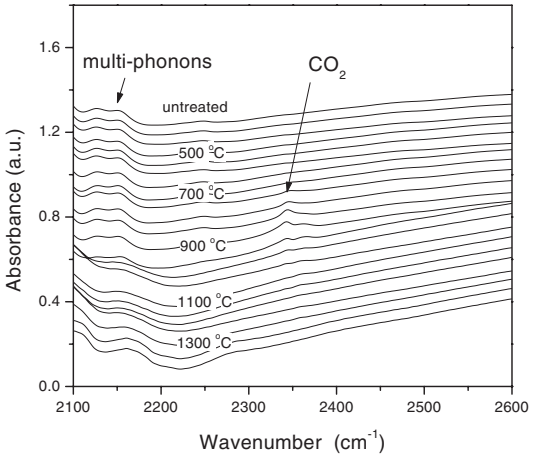

FIGURE 6. CO_2 features detected between 600 and 1300 °C (data from thin sections of LHC01). The spectra are shifted for clarity.

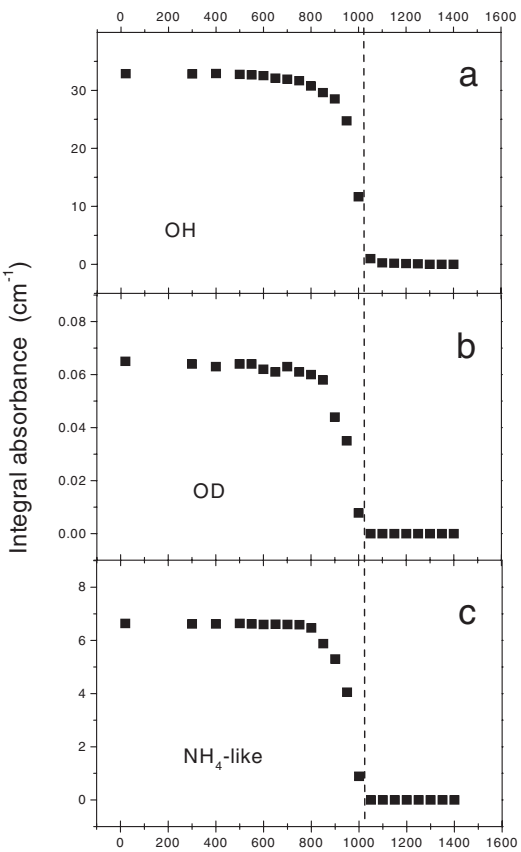

FIGURE 7. Integral absorbance of different species as a function of temperature: (**a**) OH species, (**b**) OD species, and (**c**) NH_4-like species.

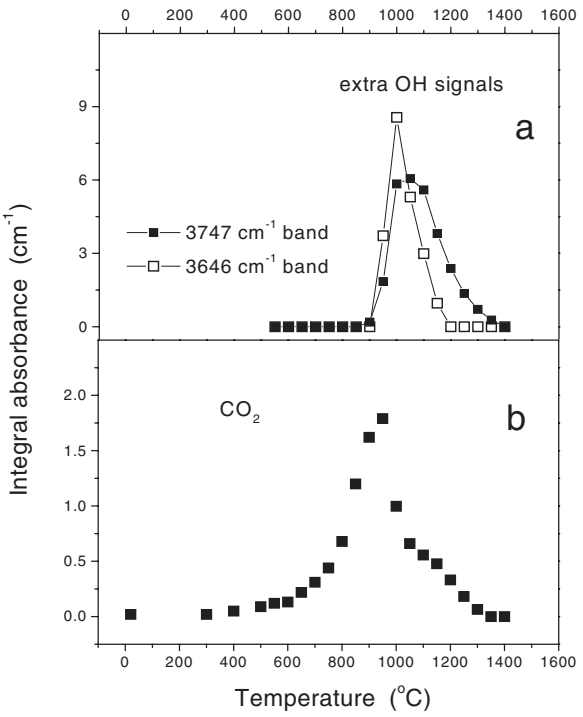

FIGURE 8. Integral absorbance of additional species formed in annealed talc as a function of temperature: (**a**) OH species and (**b**) CO_2.

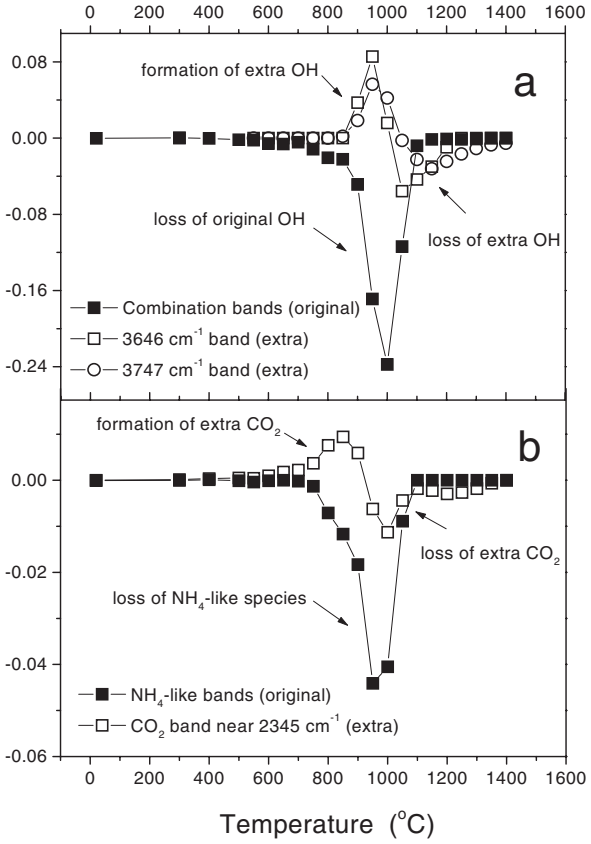

FIGURE 9. Changes (derivative) of integrated absorbance as a function of temperature: (**a**) original and extra OH species, and (**b**) NH_4-like and CO_2 species.

suggests that one should use the absorption intensity of first or second overtone bands with care in calculating the contents of OH in talc heated at very high temperatures.

We found that, like sericite (Zhang et al. 2005), the frequency of the OH bands obtained from the quenched talc did not show a significant change in frequency during dehydroxylation (Fig. 2a). For example, the positions of the OH bands near 3676 and 3660 cm^{-1} remain almost unchanged in samples annealed below 800 °C. A small increase (about 1–2 cm^{-1}) in frequency was detected in the samples heated at 900 °C. This implies that in the quenched materials weakening of the O-H bonding did not occur until very close to the main dehydroxylation. An absorption feature near 2345 cm^{-1} was recorded in the samples treated at about 600 °C (Fig. 6). This band gained its intensity on further heating to 950 °C. On further heating, it showed a decrease in intensity from 950 to 1300 °C. Finally it became undetectable above 1300 °C (Figs. 8b and 9b). This band is assigned as the absorption of CO_2. Similar features have been seen in other heated pyrophyllites and mica (Wang et al. 2003; Zhang et al. 2005).

Dehydroxylation of talc is accompanied by dramatic structural changes and thermal decomposition. The samples annealed between 1000 and 1100 °C show IR spectra (between 20 and 1500 cm^{-1}) very different from that of the untreated talc (Figs. 1a and 1b). The bands associated with stretching vibrations of SiO_4 are significantly affected by the structural modifications (Fig. 1b). Apparently, the SiO_4 groups must form new linkages, which changes the local symmetry and gives rise to several additional bands between 800 and 1300 cm^{-1}. The significant differences of the overall spectral patterns between untreated and dehydroxylated talc indicate that the layer structure of talc is destroyed in talc dehydroxylate. This is further supported by the featureless spectra in the frequency region between 20 and 200 cm^{-1}, in which bands related to interlayer vibrations commonly occur. The structural changes can be also seen in the wavenumber region of 1600–2200 cm^{-1}, where the multi-phonon bands of Si-O vibrations located. We noted that the spectrum of powdered samples annealed at 900 °C showed characteristic bands of talc with much weaker intensity than those from thin sections annealed at the same temperature, indicating more percentage of the talc phase (Figs. 1a, 1b, and 6). This difference is attributed to the observation that dehydroxylation is a kinetic process and is affected not only by temperature, but also by grain size and annealing time. For the purpose of phase identification, we examined the spectral similarities and differences among the decomposed samples, SiO_2 and pyroxene (enstatite, $MgSiO_3$) materials. Figure 10a shows IR spectra of orthoenstatite, glassy or disordered SiO_2 and dehydroxylated talc. The spectrum of enstatite shown in Figure 10a is from a sample containing 20% mol of Fe (Tarantino et al. 2002b). The spectrum was chosen because of its general features which closely match those of talc dehydroxylate, although the talc dehydroxylate in the present study has a lower Fe content. Spectral subtraction was conducted to check or remove the presence of disordered SiO_2 and

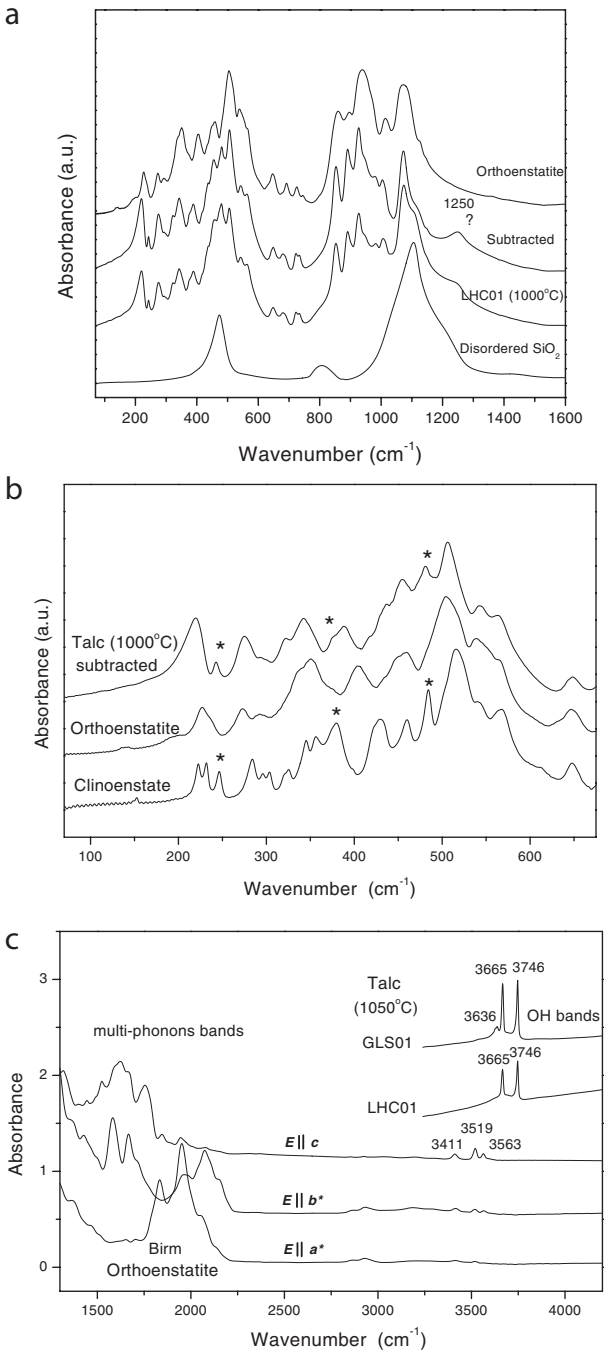

FIGURE 10. Comparisons of IR spectrum of the heated talc with those of enstatites. (**a**) Phonon spectra (70–1600 cm^{-1}) of glassy SiO_2, the talc dehydroxylate heated at 1000 °C, and orthoenstatite. The "subtracted" spectrum indicates that of talc dehydroxylate heated at 1000 °C from which the signal of SiO_2 glass is removed. (**b**) The Far-IR spectra (70–675 cm^{-1}) of heated talc (features of SiO_2 glass is subtracted), clinoenstatite and orthoenstatite (En100). The spectra of clinoenstatite and orthoenstatite are after Boffa Ballaran et al. (2001), and Tarantino et al. (2002b), respectively. The star symbols indicate the characteristic bands of clinoenstatite. (**c**) OH spectra of orthoenstatite (sample Birm with a thickness of 80 μm) and dehydroxylated talc (LHC01 and GLS01, 330 μm thick, heated at 1050 °C). The spectra are shifted for clarity.

extract the spectral pattern of other possible phases. The analysis shown in Figure 10a indicates that the subtracted spectrum of talc dehydroxylate has IR features which match very well those of orthoenstatite ($MgSiO_3$, space group *Pbca*), except for a few IR bands in the FIR region. As reported by different studies (e.g., Boffa Ballaran et al. 2001; Chihara et al. 2002; Tarantino et al. 2002b), orthoenstatite and clinoenstatite show very similar spectral features between 500 and 1400. The main spectral differences can be seen in bands located in the FIR region. The FIR spectra of talc dehydroxylate, orthoenstatite and clinoenstatite are shown in Figure 10b for a better comparison. Our analysis shows that apart from the signals of orthoenstatite, the characteristic bands (those bands near 246, 378, and 484 cm^{-1} as indicated by star symbols in Fig. 10b) of clinoenstatite ($MgSiO_3$, space group $P2_1/c$) are present in the talc dehydroxylate. These observations indicate the decomposition of talc into $MgSiO_3$ materials (both orthoenstatite and clinoenstatite) and amorphous SiO_2. A single crystal of orthoenstatite (sample Birm) was measured to further compare the OH species in the decomposed talc and pyroxene. The orthoenstatite sample exhibits three O-H stretching bands at 3411, 3519, and 3563 cm^{-1}, mainly vibrating along the c axis (Fig. 10c). These bands are not observed in the partially or fully dehydroxylated talc.

Results of in situ IR measurements

In situ IR absorption measurements on thin sections of talc GLS01 were carried out to further investigate the effect of temperature on the possible weakening of O-H bond and thermodynamics (Fig. 11). Thin sections samples were heated under vacuum to 740 °C (as talc became less and less IR-transparent on heating, it was difficult to record IR absorption spectra above this temperature) in the sample chamber of the 113v IR spectrometer. The measurements were performed on samples with different thicknesses (160, 240, and 330 μm) to maximize signal-to-noise ratios for different species. Data collections were done on both heating and cooling. The data from samples with different thicknesses exhibited essentially similar thermal behaviors, and the number of heating cycles in the temperature region appears to have little effect on the temperature evolution of the spectra. We found that the effect of increasing temperature on the frequencies of OH species is relatively weak in the measured temperature region. The main absorption band of the hydroxyl near 3676 cm^{-1} and the 3660 cm^{-1} band showed linear decreases in frequency and shifted to 3666 cm^{-1} (a change of 10 cm^{-1}, or 0.27%) and 3648 cm^{-1} (0.33%) at 700 °C, respectively (Table 2). The frequency variations are about 1.5 and 1.8 cm^{-1} per hundred degrees. The weak O-D stretching band near 2710 cm^{-1} showed similar variations: a decrease in frequency to 2700 cm^{-1} (0.37%) at 700 °C. The OH combination bands near 4055, 4182, 4323, and 4369 cm^{-1} decreased in frequency to 4041 (a change of 0.35%), 4164 (0.43%), 4305 (0.42%), and 4345 cm^{-1} (0.55%) at 700 °C. As band frequencies are directly associated with bond strength, these relatively small changes indicate that significant weakening of the O-H bonds did not occur until very close to the dehydroxylation temperature. In fact, these frequency decreases are likely due to thermal expansion of the material as vibrations of lattice phonons exhibit stronger temperature dependences. The effect of heating on the lattices is shown by the

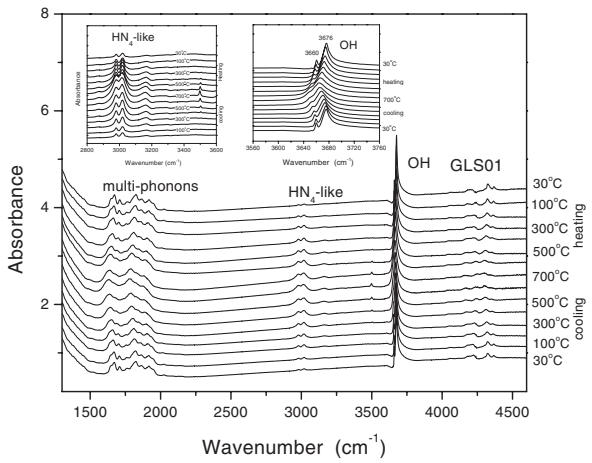

FIGURE 11. IR spectra between 1300 and 4600 cm^{-1} of talc (thin section of GLS01) from in situ measurements. The spectra are shifted for clarity. The OH band near 3676 cm^{-1} shifted to 3666 cm^{-1} (a change of 0.27%) at 700 °C. An extra OH band near 3500 cm^{-1}, which was not observed in the quenched samples, appeared on heating.

spectral changes of the multi-phonon bands between 1500 and 2100 cm^{-1}. For example, the 1824 and 1917 cm^{-1} bands, whose frequencies indicate that they are overtones of Si-O stretching vibrations, shifted to 1781 (a change of 43 cm^{-1}, or 2.4%) and 1880 cm^{-1} (37 cm^{-1}, or 1.9%), respectively (Table 2).

The in situ measurements also revealed several interesting spectral variations that we could not observe in the quenched samples. First, an extra feature near 3509 cm^{-1} appeared at 200 °C. The band might have existed at lower temperatures, but its low intensity prevented it from being resolved. It gained intensity on further heating and shifted almost linearly to 3497 cm^{-1} at 700 °C. The results reveal thermally induced proton migrations in talc. Second, the bands near 2980, 3020, 3048, and 3169 cm^{-1} (the frequency values at room temperature) showed an unexpected increase in absorbance on heating, although their frequencies exhibited weak changes (a decrease of a couple of cm^{-1} at 700 °C). These changes are reversible on cooling (Fig. 11). These bands showed similar thermal behaviors, suggesting that they are due to vibrations of similar species. Their behavior led us suspect whether they are due to multiphonon vibrations or strongly bonded OH species. Third, in situ experiments did not reveal the formation of CO_2 features near 2345 cm^{-1} at temperature as high as 740 °C, although the species appeared in quenched sample annealed at 600 °C in air. Fourth, sample GLS01 used in the in situ vacuum measurements did not show significant changes in color, whereas, the quenched samples annealed above 600 °C are slightly white or gray white, although the starting GLS01 was gently light green. This difference indicates that possible oxidation of some cations existing as chemical impurities could occur when samples are heated in air.

DISCUSSION

The dehydroxylation process shown by OH species (Figs. 7a and 9a) is essentially consistent with the thermogravimetric measurements of Ward (1975), whose Figure 3 showed that the decrease in weight starts near 750 °C, resulting in a ~4% loss between 750 and 900 °C, and a further ~0.5% weight loss (at a much slower rate) between 900 and 1100 °C. The dramatic decrease in weight recorded by the thermogravimetric measurements is associated with the loss of OH, OD, and possibly NH_4 (i.e., dehydroxylation and de-ammoniation), which is shown by the decrease in intensity of these IR features near 900 °C (Fig. 7a–7c). However, not all of the original hydrogen is driven out of the material, as additional OH species were found in the decomposed talc. Heating from 900 to 1100 °C leads to the further dehydroxylation of these extra OH species. The much slower rate between 900 and 1100 °C found by the thermogravimetric measurements could be due to the loss of extra OH and CO_2 species that formed during dehydroxylation (Figs. 8a and 8b), as well as the further dehydroxylation of the remaining part of the original OH and NH_4-like species. The detailed changes of these original and thermally induced species are shown clearly in Figure 9. According to our IR data on the thin section samples, the whole dehydroxylation process finishes at temperatures as high as 1300 °C. One interesting issue related to this observation is the location of the additional OH species found in the partially dehydroxylated samples and the relationship of these species to the dehydroxylated and decomposed phases. The possible phases that might accommodate these species are (1) a partially dehydroxylated talc phase that has a defective or disordered talc crystal structure, (2) the decomposition-produced enstatite phases, (3) SiO_2 phases, or (4) the boundaries between some of these phases. However, the persistence of these OH bands at temperatures as high as 1200–1300 °C does not favor the idea that the additional species are located in partially dehydroxylated talc phases with a defective crystal structure, as samples heated to these temperatures did not show detectable features of talc.

The general similarities between the spectral patterns of the decomposed samples and orthoenstatite suggest that the dehydroxylated talc formed above 900 and 1100 °C has an enstatite($MgSiO_3$)-like structure. However, the IR subtracted spectrum, in which SiO_2 has been removed, is clearly different from that of the well-crystallized pure synthetic orthoenstatite (Fig. 10a) in terms of band positions and bandwidths. When compared to the pure enstatite samples, the talc dehydroxylate exhibits relatively broad FIR features and band positions with slightly low wavenumber values. Furthermore, the decomposed sample exhibits a featureless spectrum below 150 cm^{-1}. These variations could result from poor crystallization and a defective structure for the orthoenstatite phase in talc dehydroxylate. The appearance of a broad feature at wavenumbers as high as near 1253 cm^{-1} is interesting. It is probably due to a new Si-O stretching band, but its frequency is too high for common frameworks of silicates and glassy silica and silicates. This finding appears to indicate the coexistence of another phase with low-dimension structures in the treated samples, as the Si-O vibrations from common frameworks are located in a lower frequency region. The broad feature suggests it is disordered in nature.

The results in Figure 8b show that the intensity of CO_2 reaches its maximum near 1000 °C, where dehydration shows the largest intensity loss rate (first derivative of band area) (Figs. 9a and 9b). One interesting question related to this observation is whether the dehydroxylation and CO_2 incorporation, two processes with different reaction mechanisms, could affect or be related to each

TABLE 2. Frequencies or peak positions (cm^{-1}) of some IR bands observed between 30 and 700 °C from in situ measurements

Temperature (°C)	30	100	200	300	400	500	600	700	Assignment
Position (cm^{-1})	1673	1670	1665	1660	1654	1648	1640	1632	Combinations and
	1708	1705	1702	1697	1691	1685	1679	1673	overtones of Si-O
	1824	1821	1814	1809	1802	1791	1789	1781	vibrations
	1917	1915	1910	1904	1898	1892	1886	1880	Overtones of Si-O
	2024	2020	2013	2007	2003	1996	1990	1984	stretching bands
	2710	2709	2708	2706	2705	2704	2702	2700	Mg_3OD
	2980	2980	2979	2979	2978	2977	2976	2975	Stretching bands of
	3020	3020	3019	3019	3018	3017	3016	3015	NH_4 or OH?
	3169	3168	3167	3166	3164	3163	3162	3160	OH or NH_3?
			3509	3507	3504	3502	3500	3497	Extra O-H stretch
	3660	3659	3657	3656	3654	3652	3650	3648	(Mg_2, Fe)OH
	3676	3675	3673	3672	3671	3670	3668	3666	Mg_3OH
	4182	4179	4177	4175	4172	4170	4167	4164	Combinations of
	4323	4321	4318	4316	4314	4311	4308	4305	OH species
	4369	4367	4363	4359	4356	4352	4348	4345	

other. Our observation suggests that although the two processes are different, they are somehow correlated in the heated talc; i.e., carbonization appears enhanced by dehydroxylation. Similar correlation has been seen in heated mica for which the two processes take place near 700 °C, a much lower temperature. We believe that the CO_2 is very likely to be located in the interlayers, cavities and grain boundaries. However, the two processes are not interdependent. Although the CO_2 and additional OH species are found at high temperatures, the CO_2 features appeared around 600 °C, whereas the new OH bands near 3655 and 3745 cm^{-1} became detectable on approaching 900 °C. This observation indicates that the CO_2 is probably not associated with (or stabilizes) these extra OH species. Although the occurrence of CO_2 has been observed in heated pyrophyllite (Wang et al. 2003) and sericite (Zhang et al. 2005), the origin of carbon substances was unclear prior to the present study. It had been suggested that they could result from the decomposition of CO_3 and CH_n groups existing in the starting materials or diffusion of carbon-related substances during firing (Zhang et al. 2005). In the present study, the in situ heating measurements, which were carried out in vacuum, did not detect CO_2 at temperatures as high as 740 °C, in contrast to the behaviors of the quenched samples annealed in air. This indicates that the carbon substances in the quenched talc samples are mainly from external sources (most likely atmospheric CO_2). During dehydroxylation these substances could enter the fired material via the same conduits through which the H_2O was released, or through the sheets. The diffusion of external substances into the samples could complicate the data interpretation associated with thermogravimetric measurements of talc.

The appearance of the NH_4^+-like species in talc is surprising because of the crystal chemistry of talc and the lack of previous observations of the species. In general, NH_4^+ is chemically bound to either inorganic or organic molecules and is commonly released during hydrolysis to NH_3. It has been reported in other layer silicates (see an earlier section). In phyllosilicates, NH_4^+ commonly replaces monovalent cations in the crystal structure. For instance, NH_4^+ in muscovite replaces K^+ and is located in the interlayers. However, as ideal talc, $Mg_3(Si_2O_5)_2(OH)_2$, does not consist of monovalent cations, the common substitution of monovalent cations by NH_4^+ in other phyllosilicates might not be appropriate for talc. Robert et al. (1983) pointed out that in trioctahedral micas some Li^+ did not replace K^+, but in the interlayer space, i.e., it was located out of the alkaline cation sites and entered the pseudo-octahedral cavities limited by the triangular bases of two tetrahedrons of two consecutive sheets. If this is the similar case for NH_4^+ in talc, a trioctahedral phyllosilicate, the systematic increase in intensity of these species observed from in situ measurements probably indicates a change of local configuration associated with the interlayer on heating. We are surprised by the observation that both de-ammoniation and dehydroxylation processes in talc take place at temperatures as high as about 850–900 °C (Figs. 7a–7c). Although Likhacheva et al. (2004) have reported that de-ammoniation and dehydroxylation process occur in parallel in NH_4-analcime, the reported de-ammoniation occurs near 520 °C, about 300–400 °C lower than the process in talc. As OH and NH_4 are unlikely to have similar bond strengths, it is puzzling why these two very different species start to decompose or break down around the same temperature. We believe that the two processes in talc do not take place coincidently in the same temperature region, as in the case of analcime (Likhacheva et al. 2004). Pérez-Rodríguez et al. (2004) reported that in NH_4-vermiculite de-ammoniation occurred before dehydroxylation on heating and the NH_3 removal triggered the H_2O release. Given the low concentration (tens to hundreds ppm) of NH_4 ions in the two samples, their presence in talc is unlikely to play important role in the crystal structure of talc, and their decomposition is unlikely to trigger the dehydroxylation. If the two processes are dependent, it is more likely that dehydroxylation is the more important part. However, the lack of evidence for significant weakening of OH bonding at temperatures very close to dehydroxylation brings into question the driving force of the dehydroxylation in talc and its impact on other processes. It is possible that all the processes (dehydroxylation, de-ammoniation, and decomposition) take place simultaneously as a direct result of heat-triggered structural instability or break down of the crystal structure of talc. Because the IR bands associated with Mg-O, SiO_4, OH, OD, and NH_4 vibrations all show a similar behavior on heating, it is impossible to distinguish which species breaks down first and potentially initializes these processes. In other words, dehydroxylation, de-ammoniation, and decomposition in talc may be associated with local structure, lattice perfection and electron states. Therefore, variations of chemical composition, local defects, valence states of cations, and grain size could all affect the temperature and the

rate of dehydroxylation to different degrees.

Our in situ measurements result in some findings that cannot be revealed by the quench experiments. The development of the extra OH band near 3500 cm^{-1} on heating (Fig. 11) and the increase in absorbance for the bands near 2980, 3020, 3048, and 3169 cm^{-1} are interesting. The findings indicate that complex changes at the atomic level take place on heating, and new local sites and hydrogen or proton migrations must occur. The differences revealed by the two experimental approaches (quenched and in situ) are of importance. The results obtained by in situ measurements reveal the thermodynamic behavior of talc. The in situ spectra show that some OH species formed at high temperatures are not quenchable. Furthermore, heating in vacuum and in air may result in the formation of different substances (e.g., CO_2) and charge states. Careful investigations under controlled atmospheres and at in situ conditions are desirable and important for studying the dehydroxylation mechanisms in layer silicates and clay minerals. Our in situ data also show that OH bands of talc generally exhibit relatively weak changes in frequency, in contrast to those of vibrational bands related to Si-O bonds. For thermally induced dehydroxylation, it is generally accepted that increasing temperature leads to a dramatic weakening of the bond strength or an increase of the bond length between O and H, and eventually the breaking of the O-H bond must occur during the dehydroxylation. This has been commonly regarded as the driving force for the process. Note that the change in frequency of OH bands is about one order of magnitude smaller than those of framework phonons, and more importantly, the OH bands show a decrease in frequency with temperature. This suggests that the spectral variations revealed by in situ measurements are mainly driven by some type of structural "softening." Although weakening of O-H bond occurs at high temperatures, it seems to act in a passive manner.

ACKNOWLEDGMENTS

The authors thank Chris Hayward (University of Cambridge, U.K.) for assistance with the electron microprobe analysis and Ling Wang (Chengdu University of Technology, China) for useful discussions. The manuscript benefited significantly from reviews by Henry P. Scott and an anonymous reviewer.

REFERENCES CITED

Avgustinik, A.I. and Vigdergauz, V.S. (1948) Properties of talc during Heating. Ogneupory, 13, 218–227.

Bishop, J.L., Banin, A., Mancinelli, R.L., and Klovstad, M.R. (2002) Detection of soluble and fixed NH_4^+ in clay minerals by DTA and IR reflectance spectroscopy: a potential tool for planetary surface exploration. Planetary and Space Science, 50, 11–19.

Boffa Ballaran, T., Carpenter, M.A., and Ross, N.L. (2001) Infrared powder-absorption spectroscopy of Ca-free P21/c clinopyroxenes. Mineralogical Magazine, 65, 339–350.

Bošković, S.B., Gašić, M.Č., Nikolić, V.S., and Ristić, M.M. (1968) The structural changes of talc during heating. Proceedings of the British Ceramic Society, 10, 1–12.

Bray, H.J. and Redfern, S.A.T. (1999) Kinetics of dehydration of Ca-montmorillonite. Physics and Chemistry of Minerals, 26, 591–600.

Busigny, V., Cartigny, P., Philippot, P., and Javoy, M. (2003) Ammonium quantification in muscovite by infrared spectroscopy. Chemical Geology, 198, 21–31.

Chihara, H., Koike, C., Tsuchiyama, A., Tachibana, S. and Sakamoto, D. (2002) Compositional dependence of infrared absorption spectra of crystalline silicates. Astronomy and Astrophysics, 391, 267–273.

Drits, V.A., Besson, G., and Muller, F. (1995) An improved model for structural transformations of heat-treated aluminous dioctahedral 2:1 layer silicates. Clays and Clay Minerals, 43, 718–731.

Farmer, V.C. (1974) The layer silicates. In V.C. Farmer, Ed., The Infrared Spectra of Minerals, p. 331–364. Mineralogical Society, London.

Farmer, V.C. and Russell, J.D. (1964) The infra-red spectra of layer silicates. Spectrochimica Acta, 20, 1149–1179.

Ferrage, E., Martin, F., Petit, S., Pejo-Soucaille, S., Micoud, P., Fourty, G., Ferret, J., Salvi, S., de Parseval, P. and Fortune, J.P. (2003) Evaluation of talc morphology using FTIR and H/D substitution. Clay Minerals, 38, 141–150.

Fitzgerald, J.J., Hamza, A.I., Dec, S.F., and Bronnimann, C.E. (1996) Solid-state ^{27}Al and ^{29}Si NMR and ^{1}H CRAMPS studies of the 2:1 phyllosilicate pyrophyllite. Journal of Physical Chemistry, 100, 17351–17360.

Guggenheim, S., Chang, Y.-H., and Koster van Groos, A.F. (1987) Muscovite dehydroxylation: High-temperature studies. American Mineralogist, 72, 537–550.

Ishii, M., Shimanouchi, T., and Nakahirea, M. (1967) Far infrared absorption spectra of layer silicates. Inorganica Chimica Acta, 1**,** 387–392.

Ishii, T., Furuichi, R., and Kobayashi, Y. (1974) Thermoanalytical study on the chlorination of magnesium-containing ores: An application of a simple gas-flow differential thermal analysis technique. Thermochimica Acta, 9, 39–53.

Krönert, W., Schwiete, H.E., and Suchow, A. (1964a) Das thermische Verhalten von Speckstein und die Stabilität der Magnesiummetasilikat-Modifikationen. Ziegelindustrie, 17, 364–369.

Krönert, W., Schwiete, H.E., and Suchow, A. (1964b) Über das thermische Verhalten von Speckstein und die Stabilität der $MgSiO_3$-Modifikationen. Naturwissenschaften, 51, 85–86.

Likhacheva, A.Y., Veniaminov, S.A., and Paukshtis E.A. (2004) Thermal decomposition of NH_4-analcime. Physics and Chemistry in Minerals, 31, 306–312.

MacKenzie, K.J.D., Brown, I.W.M., Meinhold, R.H., and Bowden, M.E.J. (1985) Thermal reactions of pyrophyllite studied by high-resolution solid-state ^{27}Al and ^{29}Si nuclear magnetic resonance spectroscopy. Journal of the American Ceramic Society, 68, 266–272.

Martin, F., Petit, S. Grauby, O., and Lavie, M.P. (1999) Gradual H/D substitution in synthetic germanium bearing tales: a method for infrared band assignment. Clay Minerals, 34, 365–374.

Muller, F., Drits, V., Plancon, A., and Robert, J.L. (2000) Structural Transformation of 2:1 dioctahedral layer silicates during dehydroxylation-rehydroxylation reactions. Clays and Clay Minerals, 48, 572–585.

Pérez-Rodríguez, J.L., Poyato, J., Jiménez de Hharo, M.C., Pérez-Maqueda, and Lerf, A. (2004) Thermal decomposition of NH_4^+-vermiculite from Santa Olalla (Huelva, Span) and its relation to the metal ion distribution in the octahedral sheet. Physics and Chemistry in Minerals, 31, 415–420.

Petit, S., Martin, F., Wieqiora, A., de Parseval, P. and Decarreau, A. (2004) Crystal-chemistry of talc: A near infrared (NIR) spectroscopy study. American Mineralogist, 89, 319–326.

Pironon, J., Pelletier, M., De Donato, P. and Mosser-Ruck, R. (2003) Characterization of smectite and illite by FTIR spectroscopy of interlayer NH_4^+ cations. Clay Minerals, 38, 201–211.

Robert J.-L., Volfinger, M., Barrandon, J.-N., and Basutęu M. (1983) Lithium in the interlayer space of synthetic trioctahedral micas. Chemical Geology, 40, 337–351.

Russell, J.D., Farmer, V.C. and Velde, B. (1970) Replacement of OH by OD in layer silicates and identification of the vibrations of these groups in infrared spectra. Mineralogical Magazine, 37, 869–879.

Sainz-Díaz, C.I., Escamilla-Roa, E., and Hernández-Laguna, A. (2004) Pyrophyllite dehydroxylation process by First Principle calculations. American Mineralogist, 89, 1092–1100.

Tarantino, S.C., Domeneghetti, M.C., Carpenter, M.A., Shaw, C.J.S., and Tazzoli, V. (2002a) Mixing properties of the enstatite-ferrosilite solid solution: I. A macroscopic perspective. European Journal of Mineralogy, 14, 525–536.

Tarantino, S.C., Boffa Ballaran, T., Carpenter, M.A., Domeneghetti, M.C., and Tazzoli, V. (2002b) Mixing properties of the enstatite-ferrosilite solid solution: II A microscopic perspective. European Journal of Mineralogy, 14, 537–547.

Wang, L., Zhang, M., Redfern, S.A.T., and Zhang, Z.Y. (2002) Dehydroxylation and transformations of the 2:1 phyllosilicate pyrophyllite at elevated temperatures: An infrared spectroscopic study. Clays and Clay Minerals, 50, 272–283.

Wang, L., Zhang, M., and Redfern, S.A.T. (2003) Infrared study of CO_2 incorporation into pyrophyllite [$Al_2Si_4O_{10}(OH)_2$] during dehydroxylation. Clays and Clay Minerals, 51, 439–444.

Ward, J.R. (1975) Kinetics of talc dehydroxylation. Thermochimica Acta, 13, 7–14.

Wesolowski, M. (1984) Thermal decomposition of talc: a review. Thermochimica Acta, 78, 395–421.

Wilkins, R.W.T. and Ito, J. (1967) Infrared spectra of some synthetic talc. American Mineralogist, 52, 1649–1661.

Zhang, M., Wruck, B., Graeme-Barber, A., Salje, E.K.H., and Carpenter, M.A. (1996) Phonon spectra of alkali-feldspars: phase transitions and solid solutions. American Mineralogist, 81, 92–104.

Zhang, M., Wang, L., Hirai, S., Redfern, S.A.T., and Salje, E. K. H. (2005) Dehydroxylation and CO_2 incorporation in annealed mica (sericite): An infrared spectroscopic study. American Mineralogist, 90, 173–180.

MANUSCRIPT RECEIVED MARCH 21, 2005
MANUSCRIPT ACCEPTED DECEMBER 21, 2005
MANUSCRIPT HANDLED BY GEORGE LAGER